

Observation of the transmission of gas explosions through narrow gaps using time-resolved laser/Schlieren techniques

R. Sadanandan¹, D. Markus¹, M. Spilling¹, R. Schiessl², U. Maas², J. Olofsson³, H. Seyfried³,
M. Richter³, M. Aldén³

¹Physikalisch Technische Bundesanstalt, Bundesallee 100, 38116 Braunschweig, Germany,
(E-Mail: Rajesh.Sadanandan@ptb.de, Tel: +49 531 592 3557, Web: www.ptb.de)

² Universität Karlsruhe, Institut für Technische Thermodynamik, Kaiserstraße 12, D-76128 Karlsruhe, Germany (E-mail: schiessl@itv.uni-stuttgart.de, Tel: +49 (0)721 608 3930)

³Lund Institute of Technology, Division of Combustion Physics, S-22100 Lund, Sweden.
(E-mail: jimmy.olofsson@forbrf.lth.se, Tel: +46 (0) 46-222 03 53)

Abstract

We investigate the re-ignition of a hot exhaust gas jet impinging into unburned hydrogen/air mixture. A simple configuration is studied, where a jet of hot exhaust gases first travels through a narrow nozzle, and then impinges into an unburned H₂/air mixture, possibly initiating ignition and combustion. The investigation uses experimental observations made by recording high-speed sequences of laser-induced fluorescence (LIF) images of the hydroxyl-radical (OH) as well as detailed numerical simulations of the involved processes of molecular mixing and chemical reactions. The importance of the hot jet temperature and the speed of molecular mixing is examined. Simulations unveil the information that can be derived by the observation of the hydroxyl radical, and the actual observations are analysed in this respect. Experimental results show the quenching of the flame inside the nozzle and the subsequent ignition of the hydrogen/air mixture by the hot free jet, and reveal that the ignition and combustion is influenced by the mixing process, which, in turn, depends on the jet velocities. These findings promote the understanding of the processes involved and allow an improvement of the protection type flameproof enclosures.

Introduction

The use of electrical equipments in explosive environments demands special protection in order to avoid accidental ignition of the surroundings. The protection type “flameproof enclosure” keeps potential ignition sources (electrical and non-electrical) inside housings, which can withstand an internal explosion of gas/air mixtures. However, ignition of the explosive gases in the outer atmosphere may take place due to a hot jet escaping from these enclosures through the inevitable gaps, like the ones present at the shaft bearing of an electrical motor. Observations have shown that this process involves a quite complex interplay of physical and chemical processes and demands detailed investigation in order to be comprehended; ultimately, the goal is to develop a reliable numerical model that can predict the re-ignition properties of a given configuration.

The present study focuses on gaining information about the fundamental mechanisms involved in this process. We studied ignition phenomena in nearly stoichiometric hydrogen/air mixtures induced by hot exhaust gas jets experimentally and numerically. Experiments were performed in an optically accessible constant-volume combustion vessel. The vessel consisted of two chambers. In one chamber, hot exhaust gas was generated by spark ignition of a hydrogen/air mixture. This gas expanded through a nozzle into a quiescent hydrogen/air mixture at atmospheric pressure and room temperature in the second chamber. The temporal development of the hot jet penetration into the unburned mixture and the distribution of the OH-radical inside the free jet flow were observed by a combined Schlieren and planar laser induced fluorescence (PLIF) visualisation. A high-speed multiple-pulse laser and detection system was used to obtain the time-resolved OH-LIF images. Using this set-up, the influence of different jet velocities on the gas expansion and ignition processes was studied by repeating the experiment with different nozzle diameters and varying the distance from the spark plug to the nozzle inlet. The Schlieren image sequence helped in studying the temporal evolution of the jet structure while the LIF images of the OH radical identified points where

combustion had occurred in time and space. Numerical simulations were performed using a zero-dimensional model and a detailed reaction mechanism.

Theoretical Background

Earlier works on explosion initiation by a hot turbulent jet done by Meyer et al. [1] and Phillips [2] emphasised the influence of mixing and chemistry on the ignition process. Moen et al. [3] carried out large-scale tests of acetylene-air mixtures into an unconfined test section to investigate the effect of obstructing the jet orifice to enhance jet mixing in the test section. They showed clearly the effect of the coupling between the rate of combustion and the degree of turbulence on the onset of violent explosions. Recent works by Krock [4] examined the initiation of explosion of hydrogen-air mixtures diluted with steam or nitrogen by using jets of hydrogen and steam. Djebaili et al. studied the ignition limits of hydrogen-air mixtures diluted with steam or carbon dioxide by hot transient jets as a function of mixture composition and initial temperature [5]. However, all the previous studies fail short of giving in depth knowledge about the fundamental mechanisms behind the ignition process that is initiated by hot burned gases. For the current work, the underlying parameters behind the ignition of combustible mixture by hot turbulent jets are acquired from the earlier experimental [6] and numerical works [7] done at Physikalisch Technische Bundesanstalt (PTB). The objective is to get empirical information about the mechanism involved in the ignition process.

The transmission of gas explosion through narrow gaps is an instationary and spatially inhomogeneous process influenced by turbulence and chemical reactions. This necessitates the use of experimental methods that can give spatially and temporally resolved information. The technique of planar laser induced fluorescence has been successfully used in highly turbulent environments due to its high sensitivity and species specificity with high spatial and temporal resolution [8,9]. One intermediate species that is produced in the reaction zone during ignition process is OH. So OH radical can be used as an indicator for the reaction zone in any ignition process and also it stands out for its relatively high concentration [10,11]. The radicals can be detected by measuring the fluorescence that follows their excitation by a laser. This paper presents the results obtained using time resolved OH planar induced fluorescence and laser Schlieren imaging of the transmission of gas explosions through narrow gaps. The OH PLIF images were used to detect the ignited locations inside the turbulent jet in space and time and the laser Schlieren images were used in studying the temporal development of the jet simultaneously. The results were compared with numerical simulations.

Simulation of Mixing and Ignition Processes

The processes occurring during the impingement of the jet into the unburnt mixture can be studied by a simple mixing model of burnt jet gases and unburnt hydrogen/air mixture. This model describes a volume of hot exhaust gas coming out of the nozzle, to which then gradually unburnt gas is mixed. During the mixing process chemical reactions occur, which possibly lead to the ignition of the volume. A burnt exhaust gas of a stoichiometric hydrogen/air mixture represents the jet. The temperature of this mixture T_b was selected as a parameter, reflecting the temperature range of 800 up to 1500 K of the jet as measured in previous work [6], and the chemical composition was set to the equilibrium composition corresponding to the selected temperatures. The unburnt gas is a stoichiometric hydrogen/air mixture at $T_u = 300\text{K}$. A homogeneous reactor model is considered, which at time $t = 0$ consists of pure burnt mixture representing the exhaust gas from the nozzle exit. According to a certain mixing rate ω_{mix} , mass of the reactor is gradually replaced by mass from the unburnt gas, until the reactor is at $t \rightarrow \infty$ entirely "filled" with mass from unburnt gases. Let ξ_u denote the mass fraction of gas originating from the initially unburned gas at a given time t . Then, the mixing process is described by $d\xi_u/dt = (1-\xi_u) \cdot \omega_{\text{mix}}$, with $\xi_u(0) = 0$. In the following, we use also the symbol ξ for ξ_u . Chemical reactions take place simultaneously to the mixing process, possibly leading to an ignition of the mixture. Chemical reactions were treated by a detailed reaction mechanism for hydrogen/air combustion, including 38 elementary reactions of 9 species. The temporal evolution of the system (described by its temperature and mole fractions at every instant of time) can be calculated by numerically solving the conservation equations for mass and energy, and calculating chemical source terms according to the reaction mechanism [12].

Experimental Set-up

Explosion vessel

In view of the complex processes associated with the ignition problem, an experimental set-up, well defined and optically accessible, is used for the current studies. The schematic of the explosion vessel is as shown in Figure 1. It consists of two vessels interconnected by means of a nozzle. The cylindrical small vessel is 80 mm in length and 60 mm in diameter leading to a volume of 0.226 litres. This vessel is flanged to the second vessel, which has a volume of 12 litres. It is provided with three quartz windows for optical access. Both the vessels are filled with 28% hydrogen/air mixtures at the beginning of each experiment. The fuel/air mixture in the first vessel is ignited by means of electrical discharges on the symmetrical axis of the vessel at a distance X_i from the inlet of the nozzle. The hot burned gases expand into the second vessel through the nozzle. The pressure rise in both the vessels is recorded by means of Kistler (Model 6031) transducers. The development of the jet structure and the subsequent ignition processes is captured at right angles to the flow by means of ICCD cameras. By repeating the experiments with different values of X_i and nozzle diameters d the influence of jet velocities on the gas expansion and ignition processes can be studied.

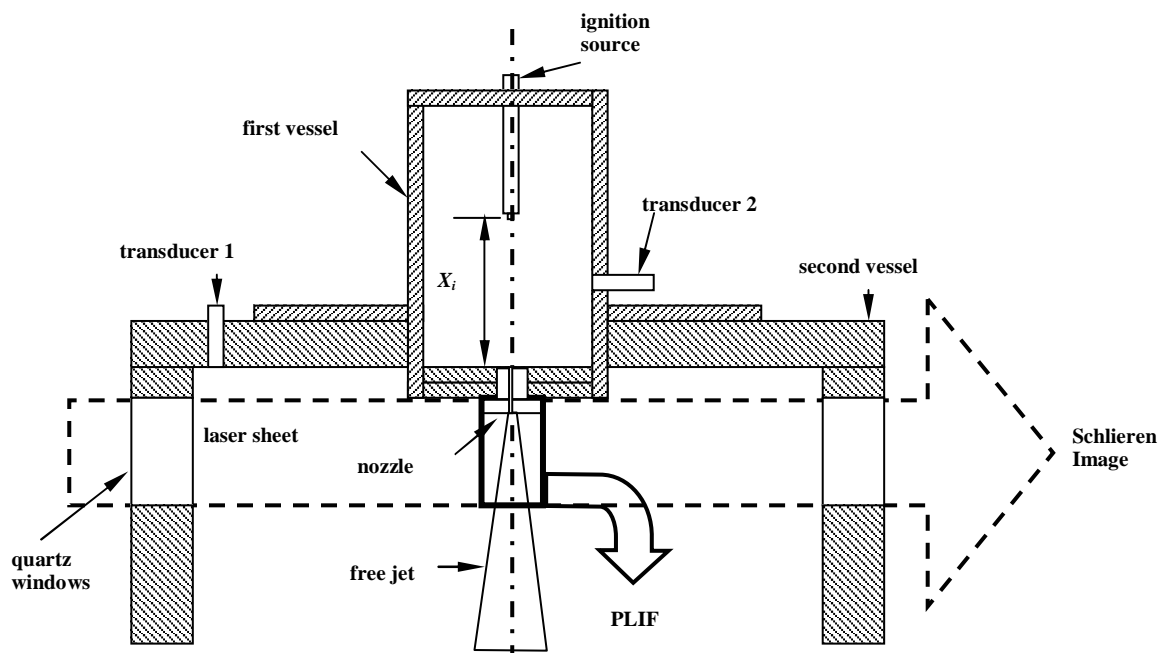


Figure 1: Schematic of the Explosion Vessel.

Optical set-up

The multiple YAG laser cluster used for the current series of OH-PLIF experiments consists of frequency doubled four standard flash lamp-pumped Nd:YAG lasers, each of them can be operated in double pulse mode with the timing between the pulses ranging from 25 μ s to 145 μ s. The exciting laser pulses for OH-PLIF were obtained using the frequency-doubled output from a dye laser operating on Rhodamine 590 dye solution pumped by the Nd:YAG laser cluster. The detector system used for the visualisation of planar OH-LIF is an ultra fast CCD camera (Imacon 468, dynamic range 8 bit, 576x385 pixels) with eight individual CCD detectors. Exposure times, gains and trigger delays are individually programmable for each CCD thus providing full timing control. The recorded images were corrected for misalignments between the eight CCD units inside the high-speed camera. More details of the laser cluster and camera can be found in [13].

For OH-PLIF a frequency doubled dye laser was tuned to the $Q_1(9)$ transition at 283 nm in the $v''=0$, $v'=1$ band of the $A^2\Sigma^+-X^2\Pi$ system. By means of cylindrical lenses the laser beam was formed into a vertical sheet of approximately 39 mm in height and 200 μ m in thickness at the viewing section. Subsequent fluorescence from the OH radical was observed using a combination of a high reflection filter (HR 275-295 nm) and a UG11 filter in front of the camera lens which also eliminate reflections

of laser light. Part of the incoming laser beam is sent to a fluorescent dye cell and the ensuing fluorescence is reflected on to the side of the same CCD as OH-LIF fluorescence. This simultaneous dye cell profile was used to correct the laser profile inhomogeneities. A portion of the output beam from the dye laser is diverted into a photodiode by means of a beam splitter. This allowed on-line monitoring of the laser pulse energies.

The laser Schlieren optical system consists of a He-Ne laser (20mW at 632.8 nm) as a point source, a beam expander for collimating the beam and a subsequent lens-knife edge combination to obtain the Schlieren image. For the laser Schlieren imaging a high speed ICCD camera (La Vision Streak Star, 13 bit dynamic range, 384x550-pixel array) coupled to a Sigma zoom lens (75-300, 4-5.6 f) was used. Four sequential Schlieren images were taken during each experiment with 50 μ s time step and 1 μ s. exposure time. The timing between the laser pulses and the different camera gate openings were adjusted by means of a delay generator circuit.

Results and Discussion

Numerical results

With the homogeneous reactor mixing model described above, setting the temperature of the burnt gas to $T_b = 1000\text{K}$ and varying the mixing rate ω_{mix} in the range of 0.01 s^{-1} up to 10^6 s^{-1} , the relationship between temperature and mixture fraction as shown in Figure 2a is obtained. At $t = 0$, the system is at the point ($\xi_u = 0, T = 1000\text{K}$), corresponding to the burnt gas from the hot jet. A pure mixing process (without any chemical reactions) is represented by a straight line through ($\xi_u = 0, T = 1000\text{K}$) and ($\xi_u = 1, T = 300\text{K}$). Exothermic chemical reactions can occur in the system for $\xi_u > 0$. These reactions cause a gradual temperature rise; however, for high mixing rates ω_{mix} the cooling of the system caused by the constant feed of unburned cold gases is faster than the rate of heating by chemical reactions, and consequently no ignition will occur: The system moves along (or at least very close to) the lower “mixing branch”. For low mixing rates ω_{mix} , the exothermic reactions heat the mixture faster than cooling by mixing occurs, and the system will eventually burn; this process corresponds to a movement along the upper branch shown in the diagram (Figure 2a). Jumps between the branches are possible (see the detail in Figure 2a). For the decision about whether the jet can cause the mixture to ignite and burn, only the values at $\xi_u \rightarrow 1$ (corresponding to the state of the system at infinite time: the stationary state) are important. The occurrence of two branches in this diagram clearly displays the effect of competing physical (mixing) and chemical (heat release by chemical reactions) processes.

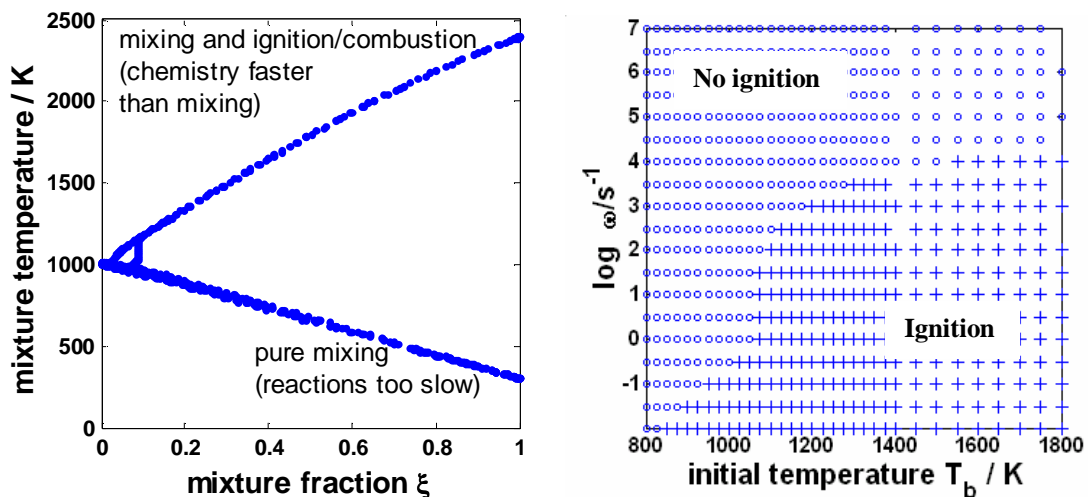


Figure 2: Left (a): Computed temperatures as a function of mixture fraction, mixing rate ω_{mix} varied in the range 0.01s^{-1} up to 10^6s^{-1} . Stationary temperature is reached for $\xi = 1$. Right (b): Behaviour of the homogeneous mixing reactor for various initial temperatures and mixing rates ω_{mix} . “o” denotes conditions where the stationary temperature (at $\xi = 1$) is $< 350\text{K}$ (no ignition), “+” denotes states where ignition occurs (stationary temperature $> 1700\text{K}$). No stationary temperatures between 300K and 1700K were obtained.

The dependence of the ignition process on the mixing rate is of course only one important parameter. The limiting parameter for the chemical processes is the temperature of the exhaust gas at the nozzle exit. This dominant influence of the temperature is shown in Figure 2b, which displays the ignition behaviour of the homogeneous mixing reactor as a function of jet temperature and mixing speed. The region marked with a '+' represents conditions under which ignition occurs. The shape of the boundary between igniting and non-igniting regions in this diagram is dominated by the temperature dependence of the underlying elementary reactions [12]. These basic considerations guide the analysis and understanding of the experimental observations.

Experimental results

Experiments were conducted for four different ignition distances $X_i = 16$ mm, 24mm, 32 mm and 56 mm. Table 1 summarises the different nozzle diameters d tested for each ignition distance X_i . Changes in X_i will lead to a corresponding change in the pressure gradient along the nozzle, thereby changing the jet velocity. Also changes in nozzle diameter will change the rate of cooling of the burned gas as it passes through the nozzle, such determining its temperature when it gets into first contact with the unburned gas. The influence of nozzle diameter and ignition distance on the ignition phenomena was the crucial part for the current experiments.

Ignition Distance X_i (mm)	Nozzle Diameter d (mm)
16	0.8
24	0.7, 0.8, 0.9
32	0.8, 0.9, 1.0
56	0.8, 1.1, 1.3

Table 1: Measurement parameters.

Figure 3 shows the simultaneous laser Schlieren and OH-PLIF images for $X_i = 32$ mm and $d = 0.8$ mm. The expansion of the hot gas jet can be seen from the Schlieren sequences in Figure 3a. The first frame is taken 2640 μ s after ignition in the first vessel. The time interval between each frame is 40 μ s. The simultaneous and time-resolved OH-PLIF images are shown in Figure 3b. The first frame of the PLIF image is taken simultaneously with the first frame of the Schlieren image. The time interval between the PLIF images is 20 μ s. Due to malfunctioning, one of the CCD units of the framing camera used for OH-PLIF was not used for the experiments. Comparison of the Schlieren/OH-PLIF and pressure data reveals that in this case there is no ignition in the second vessel. The absence of appreciable amount of OH radical at the exit shows quenching of the flame inside the nozzle before it expands into the second vessel. However, weak OH-LIF along the axis of the jet can be seen in some of the PLIF sequences from the hot burned gases in the first vessel.

The simultaneous Schlieren and OH-PLIF sequences for ignition of combustible gas by hot burned gas are shown in Figure 4a and 4b, respectively, for $X_i = 32$ mm and $d = 1.0$ mm. The first Schlieren image is captured 2540 μ s after ignition in the first vessel. The time interval between the different frames is 40 μ s. The first frame of the OH-PLIF sequence is taken approximately 2 μ s after the first Schlieren image and the time interval between the different frames in the sequence is 20 μ s. The region where combustion has occurred can be seen clearly from the sudden increase in OH-LIF intensity at $t = 2562$ μ s at a distance of approximately 9 mm in the PLIF sequences. It can be seen that the first combustion occurs well within the zone that was reached by the jet, rather than at the jet border.

The effect of changes in X_i on the ignition behaviour can be seen from the simultaneous Schlieren and OH-PLIF images on Figure 5. The results shown are for $X_i = 56$ mm and $d = 1.1$ mm. The first frame in the Schlieren sequence is taken 3450 μ s after ignition in the first vessel. The successive frames are taken with a time interval of 40 μ s. The first PLIF image is taken approximately 2 μ s after the first Schlieren image. Ignition of the explosive gases by the hot jet happens in the time interval between the first and second Schlieren images, as can be seen from the first 3 images of the PLIF sequence. The imaged area starts at a distance of 29 mm from the exit of the nozzle. Again, the ignition seems to start at the tip of the jet rather than the sides. The successive images show the growth of the ignition kernel. The interaction between a turbulent flow field and the combustion process is clearly seen.

Note that the turbulence was not present initially; it must have been induced by the jet. These images make clear that there is a range of mixing speeds present.

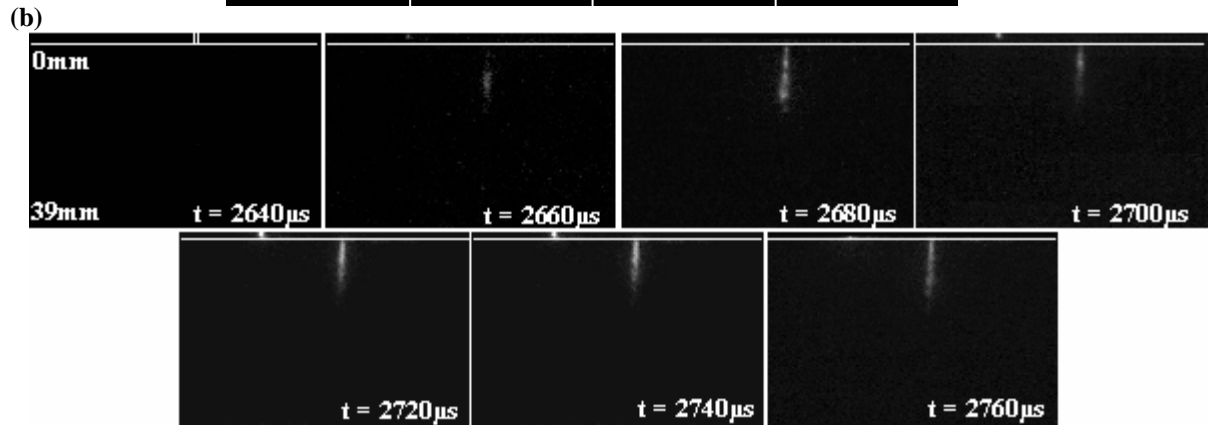
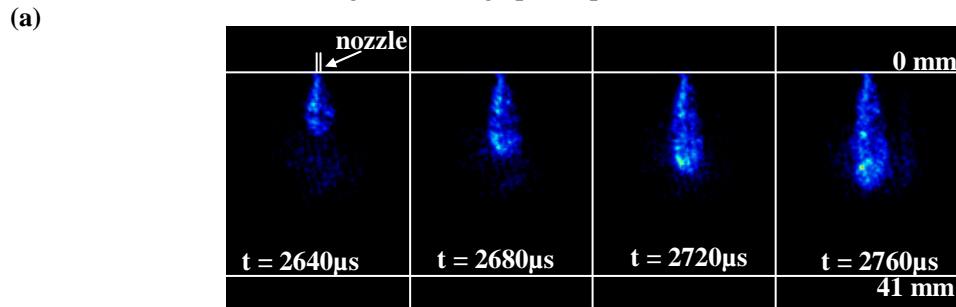


Figure 3: Ignition distance $X_i = 32$ mm, diameter of the nozzle $d = 0.8$ mm (a) Sequential laser Schlieren images; imaged area is 41×37 mm² (b) Simultaneous and time-resolved OH-PLIF images; imaged area is 39×58 mm².

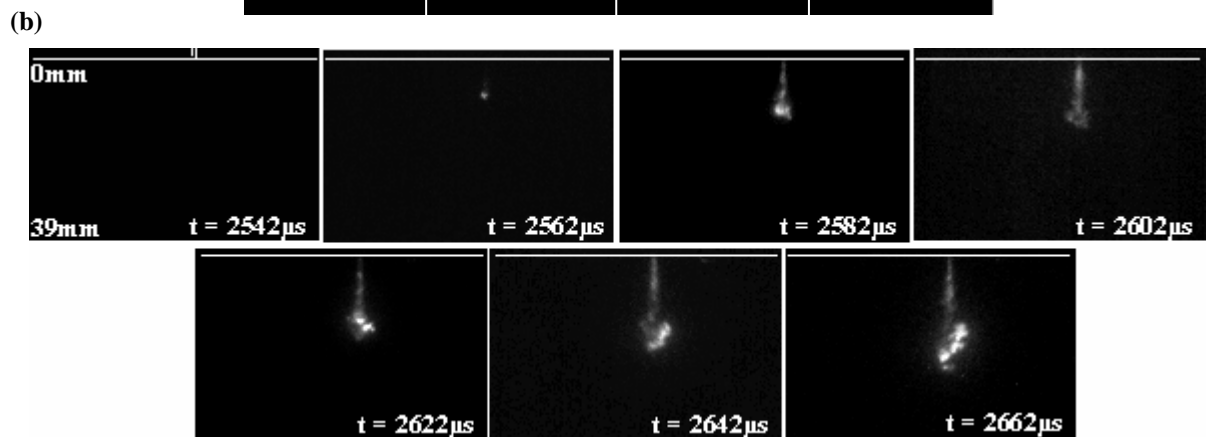
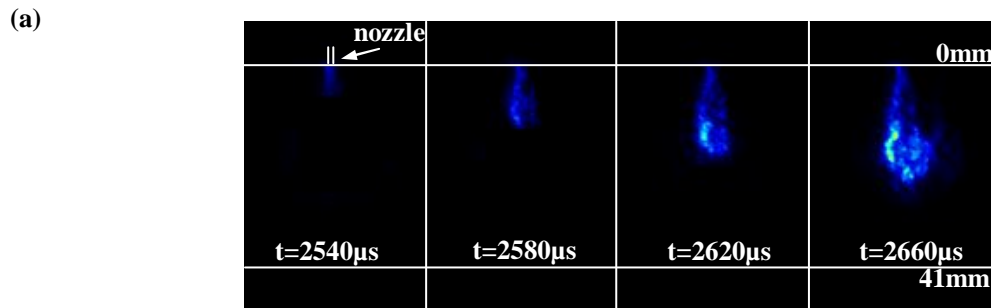


Figure 4: Ignition distance $X_i = 32$ mm, diameter of the nozzle $d = 1.0$ mm (a) Sequential laser Schlieren images; imaged area is 41×37 mm² (b) Simultaneous and time-resolved OH-PLIF images; imaged area is 39×58 mm².

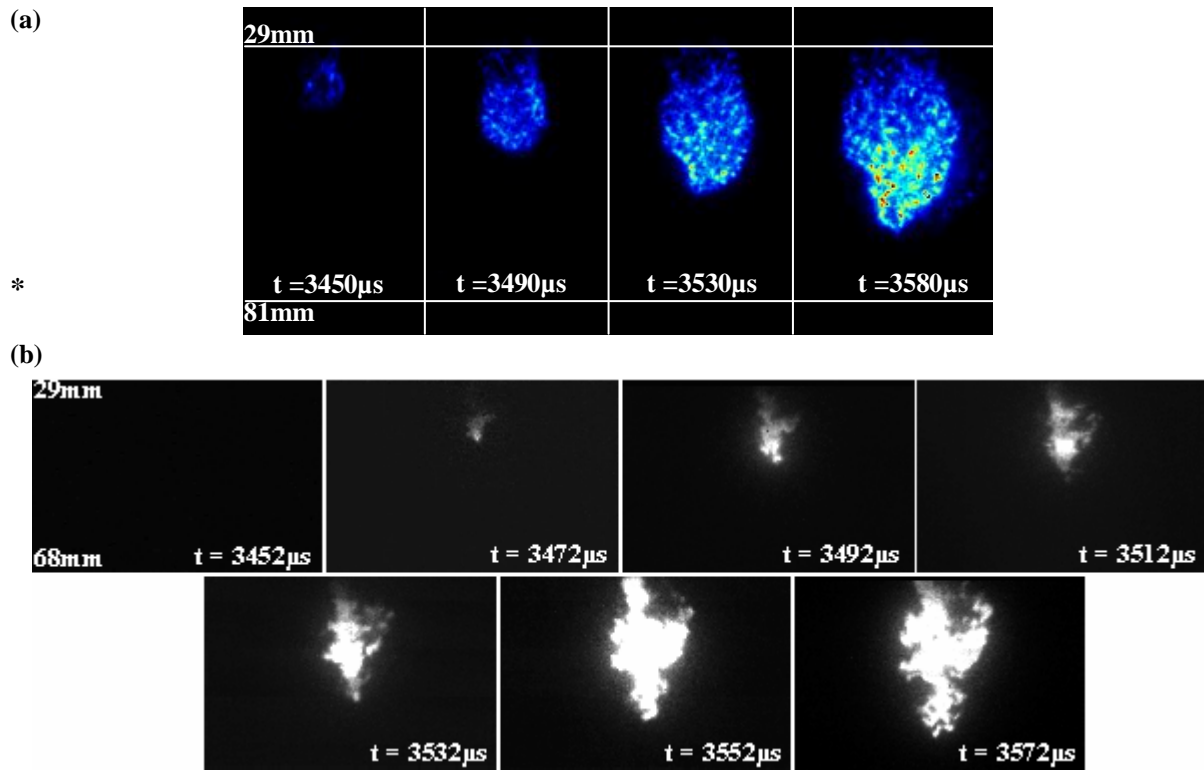


Figure 5: Ignition distance $X_i = 56$ mm, diameter of the nozzle $d = 1.1$ mm (a) Sequential laser Schlieren images; imaged area is $52 \times 37 \text{ mm}^2$ (b) Simultaneous and time-resolved OH-PLIF images; imaged area is $39 \times 58 \text{ mm}^2$.

The apparent change in ignition behaviour due to changes in X_i from 16 mm to 56 mm roots from the changes in pressure ratio across the nozzle. This in turn leads to an appreciable increase in the jet velocities. This changes further with changes in nozzle diameters. The immediate impact of these variations is on the rate of mixing between the hot and the cold gases, which evidently decides the chances of ignition, as is also evident from the numerical simulations. In our experiments, as X_i is changed from 24 mm to 56 mm, the axial distance at which ignition has occurred shifted from 6 mm to 41 mm approximately for $d = 1.1$ mm. Also for $X_i = 24$ mm the probability for 100% ignition was at $d = 0.9$ mm whereas the corresponding values for $X_i = 32$ mm and 56 mm were 1.0 and 1.3 mm respectively. For a given massflow out of the nozzle, reducing the nozzle diameter increases the jet velocity and hence the mixing rate. In the diagram shown above (Figure 2b), this corresponds to a movement vertically upwards, possibly causing a transition from the ignition-region to the area where no ignition occurs. Also, the nozzle diameter possibly affects the jet temperature at nozzle; varying the jet temperature corresponds to a horizontal movement in the diagram in Figure 2b; here, also a transition from igniting to non-igniting regions is possible.

Conclusions

This paper reports on the results of numerical studies and experimental work conducted to investigate ignition phenomena in nearly stoichiometric hydrogen/air mixtures by hot exhaust gas jets. The simulation results delivered a systematic insight into the principle effects during ignition and combustion: the competition of physical and chemical timescales was shown to play a crucial role for the ignition process. The simultaneous laser Schlieren and time resolved OH-PLIF images show the quenching of the flame inside the nozzle and the subsequent ignition of the combustible mixture by the hot exhaust jets. The change in the ignition behaviour with changes in mass flow rate and nozzle diameter indicates the influence of the mixing process and mixture temperature on the ignition process. Further work will be done to determine the mixture fraction and the instantaneous temperature profile at the time of ignition. This will be a big step forward in the improvement of the protection type flameproof enclosures.

Acknowledgements

This work was supported by a grant under the EU TMR program 'Access to Large Scale Facilities', contract number ERBFMGECT950020 (DG12), which is gratefully acknowledged.

References

1. Meyer, J.W., Urtiew, P.A., and Oppenheim, A.K.: On the inadequacy of gasdynamic processes for triggering the transition to detonation. *Comb.Flame* (1970) **14** 13-20.
2. Phillips, H.: Ignition in a transient turbulent jet of hot inert gas. *Comb. Flame* (1972) **19**, 187-195.
3. Moen, I.O., Sulmistras, A., Hjertager, B.H. and Bakke, J.R.: Turbulent flame propagation and transition to detonation in large fuel-air clouds. *Proc. Comb. Inst.* (1986) **21** 1617-1627.
4. Krok, J.C., Jet initiation of deflagration and detonation. Ph.D. thesis, California Institute of Technology, Pasadena (1997).
5. Djebaili, N., Lisabet, R., Dupre, G., and Paillard, C.: Effect of the initial temperature and composition of a hot transient jet on the ignition of H₂-air-diluent mixtures. *Proc. Comb. Inst.* (1994) **25** 1539-1545.
6. Klausmeyer, U., and Beyer, M.: Enhancement of the safety of flameproof containments by clarifying the flame transmission phenomena. *International Symposium on Hazardous, Prevention and Mitigation of Industrial Explosions* (1996).
7. Markus, D., Spilling, M., Beyer, M., and Klausmeyer, U.: Development of a numerical simulation of explosions inside containments. *Chem. Eng. Technol.* (1999) **22** 41-44.
8. Hanson, R.K.: Combustion diagnostics: Planar flow field imaging. *Proc. Comb. Inst.* (1987) **21** 1677-1691.
9. Hanson, R.K., Seitzman, J.M., and Paul, P.H.: Planar laser-fluorescence imaging of combustion gases. *Appl. Phys. B* (1990) **50** 441-454.
10. Warnatz, J., Maas, U., and Dibble, R.W.: *Combustion*. 3rd Ed., Springer Verlag, Berlin (2001).
11. Dreizler, A., Lindenmaier, S., Maas, U., Hult, J., Aldén, M., and Kaminski, C.F.: Characterisation of a spark ignition system by planar laser-induced fluorescence of OH at high repetition rates and comparison with chemical kinetic calculations. *Appl. Phys. B* (2000) **70** 287-294.
12. Maas, U., and Warnatz, J.: Ignition processes in hydrogen/air mixtures. *Comb. Flame* (1988) **74** 53-69.
13. Hult, J., Ritcher, M., Nygren, J., Aldén, M., Hultqvist, A., Christensen, M., and Johansson, B.: Application of a high-repetition-rate laser diagnostic system for single-cycle-resolved imaging in internal combustion engines. *Appl. Opt.* (2002) **41** 5002-5014.